Original Research Article

IJCRR
Section: General Science
Sci. Journal Impact Factor 4.016
ICV: 71.54

Investigations on the growth, Structural, Optical, Mechanical and Cytotoxicity Properties of a Semiorganic Single Crystal: Cytosinium Nitrate

P. Jaikumar, T. Balakrishnan, M. S. Mohamed Jaabir, S. Sakthivel

[1]PG & Research Department of Physics, National College (Autonomous), Tiruchirappalli- 620 001, Tamil Nadu, India; 2Crystal Growth Laboratory, Department of Physics, Periyar EVR College (Autonomous), Tiruchirappalli-620023, Tamil Nadu,India; [3]PG & Research Department of Biotechnology, National College (Autonomous) , Tiruchirappalli-620 001, Tamil Nadu, India; [4]PG & Research Department of Physics, Govt. Arts College (Autonomous), Karur - 639 005, Tamil Nadu, India.

ABSTRACT

Aim: To synthesize and grow pyrimidine based cytosinium nitrate single crystals and characterize the grown crystals for structural, optical, mechanical, dielectric and proliferation assay. Methodology

Cytosinium nitrate, a semi organic material was synthesized and single crystals were grown from aqueous solution employing the technique of controlled slow evaporation.

Results and Discussion: The lattice parameter of the grown crystal was determined using single crystal X – ray diffractometer. Fourier transform infrared spectral analysis is carried out to identify the functional group of the grown crystal. The grown crystals were characterized using UV – Vis – NIR and dielectric analysis. Mechanical strength was estimated using Vickers microhardness test. The crystal exhibits reverse indentation size effect and belongs to soft material category. A sharp emission peak was observed in photoluminescence spectrum at 378 nm. The anti – proliferative property of grown crystal was tested on human lung cancer cell line A549.

Conclusion: All these investigations were used to reveal the properties like structural, dielectric parameters, optical, mechanical, surface morphology and biological activity.

Key Words: Crystal growth, Optical materials, Mechanical properties, Dielectric measurements, Photoluminescence

INTRODUCTION

In the past few decades, there has been extensive investigation made in the design and characterization study of inorganic, organic and semiorganic nonlinear optical(NLO) materials [1]. Nonlinear optical materials are very significant because of its wide applications in the field of laser technology, laser communication, optoelectronic and photonic applications [2]. In particular organic materials possessing a large third – order non linearity have attracted many researchers owing to their potential application in optical switching and sensor protection [3]. Synthesis and characterization of novel materials for third order nonlinear optical application has gained much attention by the researchers [4]. Cytosine is one of the five main nucleic acids used in storing and transporting genetic information within a cell [5]. The single crystal structure of anhydrous cytosine [6] and cytosine monohydrate [7] was reported. Several researchers reported the single crystal structure of cytosine derivatives [8-11]. Most of these complexes are dealt with application of crystal engineering to active pharmaceutical and biological applications. The epigenetic mechanism such as methylation of cytosine in DNA was discussed by Plitta et al [12]. The molecular recognition of cytosine based on proton–transfer reaction elucidated by Portalone et al [13]. Kistenmacher et al [14] made systematic study on enzyme – metal – nucleic

Corresponding Author:
T. Balakrishnan, Associate Professor, Department of Physics, Periyar EVR College, Trichy, Tamilnadu, India; Tel.: +91 – 9443445535; E-mail: balacrystalgrowth@gmail.com

ISSN: 2231-2196 (Print) **ISSN:** 0975-5241 (Online) **DOI:** 10.7324/IJCRR.2017.94814

Received: 25.01.2017 **Revised:** 02.02.2017 **Accepted:** 14.02.2017

acid ternary complexes with cytosine. It is identified that cytosine may be an interesting material to optimize them for nonlinear optical limiting applications. Because the protonation of cytosine base pair carries important structural implications in crystal engineering. In particular the base pair ability known to self – assemble in acidic media. Though, the structure of cytosinium nitrate has been reported earlier [15], there are no earlier reports on the bulk crystal growth of cytosimium nitrate. In our present investigation we report the single crystal XRD, powder XRD, FTIR, UV – Vis - NIR optical analysis, photoluminescence, dielectric, Vickers microhardness, etching studies and proliferation Assay on cytosinium nitrate single crystal.

MATERIALS AND METHODS

Crystal Growth

Cytosine ($C_4H_5N_3O$) and nitric acid (HNO_3) was dissolved in deionised Millipore water at room temperature. The resultant solution was stirred well to obtain clear homogeneous solution. The prepared solution was filtered using Whatman filter paper and taken in a beaker. Beaker containing the solution was closed with perforated polythene paper and kept in an undisturbed dust free condition. Slow evaporation at room temperature yielded transparent single crystals of cytosinium nitrate (CN) of 7 mm × 2 mm × 1 mm size were harvested in a growth period of 15 days. The as grown single crystals of CN are shown in Fig. 1.

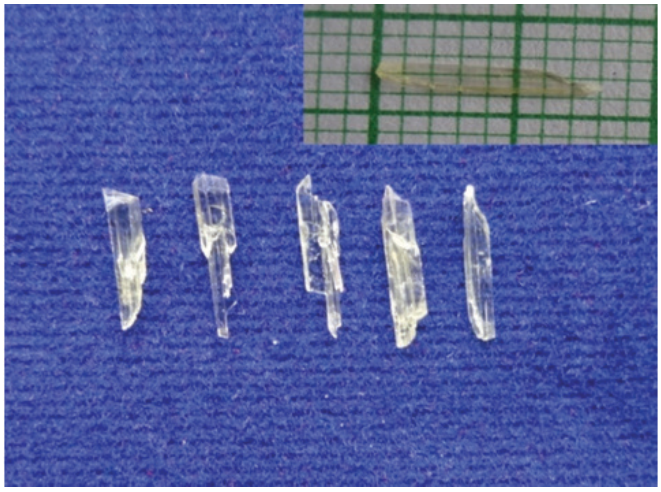

Figure 1: As grown single crystals of cytosinium nitrate.

RESULTS AND DISCUSSION

X – ray Diffraction Analysis

Single crystal X – ray diffraction data of the grown CN crystal were collected on a BRUKER NONIUS X – ray diffractometer using monochromated Cu Kα radiation (λ = 1.5408Å) at 293K. From the single crystal X – ray diffraction analysis it is confirmed that grown CN belongs to triclinic system. The obtained cell parameters are in good agreement with the corresponding reported values of Cherouana et al. [15] as is evident from Table. 1

Table 1: Crystallographic data of CN

S. No	*a* (Å)	*b* (Å)	*c* (Å)	*α* (°)	*β*(°)	γ (°)	Volume (Å^3)
1. Present work	6.509	6.726	9.222	72.02	72.85	73.75	358.9
2.Reported [15]	6.530	6.724	9.211	71.96	72.84	73.75	359.4

Powder X – ray diffraction

The powder X – ray diffraction pattern of the grown single crystal of CN was recorded on a REICH SIEFERT X – ray diffractometer instrument using Cu Kα (1.540 Å) radiation employing the reflection mode for scanning. The finely crushed sample was scanned in the 2θ values ranging from 10 – 80° at a rate of 1°/min. All the observed reflection lines were indexed with the help of computer program AUTOX 93 (Fig. 2).

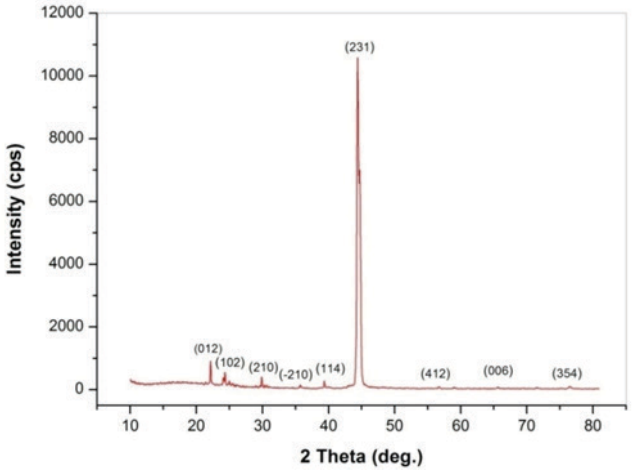

Figure 2: Powder X-ray diffraction pattern of CN.

Fourier Transform Infrared (FTIR) spectrum

In order to identify the functional groups, the FTIR spectral analysis of CN was carried out in the middle infrared region extending from 400 – 4000 cm^{-1} using a Perkin Elmer FTIR spectrometer by KBr pellet technique. The recorded FTIR spectrum is shown in Fig. 3. In the higher energy region, the NH_2 asymmetric and symmetric stretching vibrational frequencies are observed at 3342 and 3214 cm^{-1} respectively. The peak at 2932 cm^{-1} is attributed to the symmetric stretching vibration of NH. The strong band at 1728 cm^{-1} is due to the C=O stretching vibration. The NH_2 deformation and

wagging vibrations are observed at 1665 cm^{-1}. The intense peak at 1546 cm^{-1} arises due to C – NH stretching vibration. The strong band appears at 1381 cm^{-1} in the spectrum is assigned to C=C stretching vibration C–N stretching vibration observed at 1201 cm^{-1}. The peak at 792 cm^{-1} is due to the C = O bending vibration. The peaks due to NO_2 deformation are observed at 632 and 576 cm^{-1}. The prominent vibrational frequencies of FT-IR spectra with tentative assignments of CN crystal are listed in Table.2.

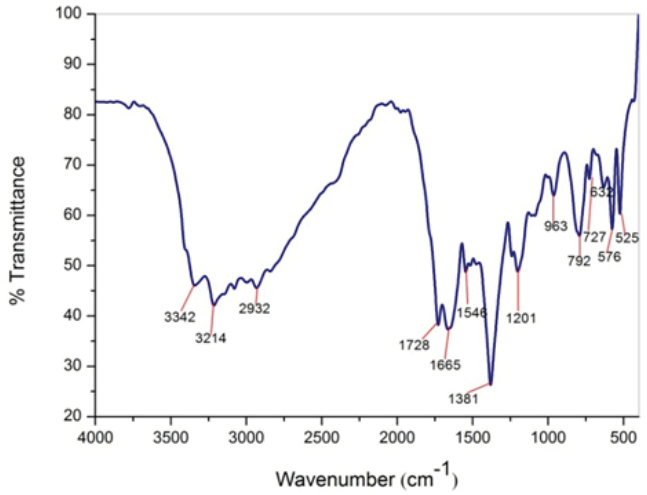

Figure 3: FT – IR spectrum of CN crystal.

Table 2: FT-IR band assignments of CN single crystal

Wave number (cm^{-1})	Assignments
3342	NH_2 asymmetric stretching vibration
3214	NH_2 symmetric stretching vibration
2932	NH symmetric stretching vibration
1728	C = O stretching vibration
1665	NH_2 deformation
1546	C – N – H stretching vibration
1381	C = C stretching vibration
1201	C – N stretching vibration
963	C – C – H deformation
792	C = O bending vibration
727	NO_2 deformation
632	–O – N = O deformation
576	–O – N = O deformation

Linear optical analysis

The UV – Vis – NIR spectrum gives more information about the band structure and optical quality of material. The absorption or emission of radiation and cut – off wavelength of grown crystals are prime factor for optical applications [16]. The UV – visible optical transmission spectrum of CN crystal was recorded between 190 – 1100 nm using Perkin – Elmer Lambda 35 spectrophotometer. The recorded transmittance spectrum of CN single crystal is shown in Fig.4. The crystal has wide transparency in the entire UV and visible region. The CN crystal is optically transparent in the entire visible region with 97% transmittance with lower cut-off wavelength of 291 nm. The optical absorption coefficient (α) was calculated using the following relation.

$$\alpha = \frac{1}{t}\log\left(\frac{1}{T}\right)$$

Where, T is the transmittance and t is the thickness of the crystal. The dependence of the optical absorption coefficient on the photon energy helps us to study the band structure and the types of transition of electrons [17]. The band gap energy of the material is calculated using the following relation

$$\alpha = \frac{A(h\upsilon - Eg)^{1/2}}{h\upsilon}$$

Where, A is a constant, E_g is optical band gap of the crystal, h is Planck's constant and υ is the frequency of the incident photon. The E_g could be estimated from the Tauc's plot of variation of $(\alpha h\upsilon)^2$ versus hυ and shown in Fig. 5. E_g is obtained from the extrapolation and interception of the linear part of the graph with X – axis [18]. The band gap energy was found to be 4.1eV. The extinction coefficient is an essential parameter to examine amount of absorption when electromagnetic waves propagates through a medium. The absorption coefficient (α) is related to the extinction coefficient K by

$$K = \lambda\alpha / 4\pi$$

Where, K is the extinction coefficient, λ is the wavelength and α is the absorption coefficient. Fig. 6 shows that variation of extinction coefficient (K) as a function of wavelength.

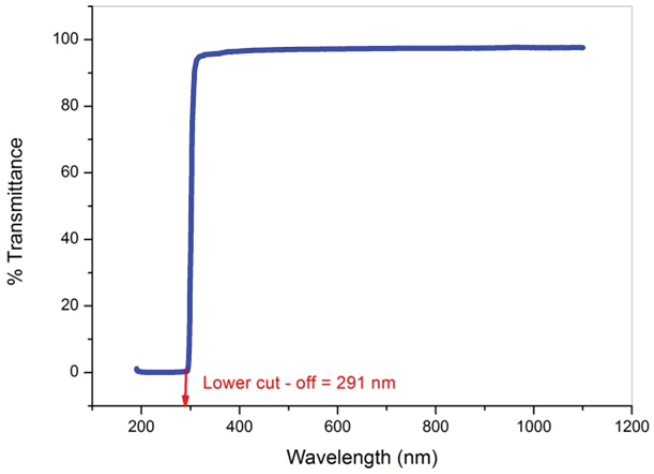

Figure 4: UV – Vis – NIR transmittance spectrum of CN crystal.

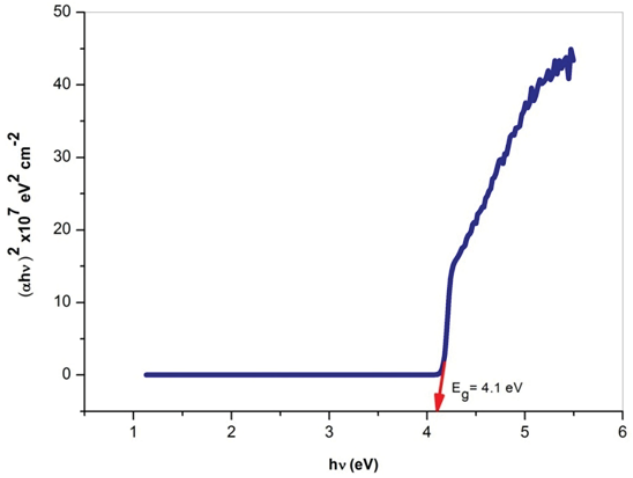

Figure 5: Plot of $(\alpha h\gamma)^2$ versus hγ of CN crystal.

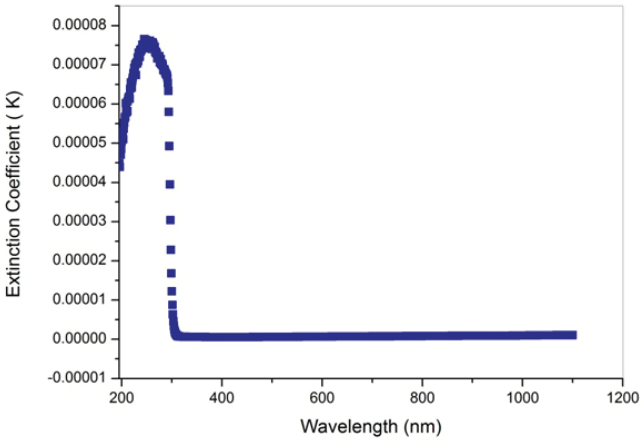

Figure 6: Dependence of extinction coefficient with wavelength of CN crystal.

Dielectric studies

The different polarization effects, relaxation phenomena and optical properties of solids can be explained by analyzing dielectric behaviour [19]. By employing the HIOKI 3536 LCR instrument the dielectric measurement were carried out on CN single crystal in the frequency region from 1 KHz to 5 MHz. Silver coated CN sample of 2mm thickness was used as the parallel plate capacitor to form dielectric medium. The capacitance of the sample was recorded by varying the frequency at different temperatures (Room temp, 50 °C, 70 °C and 90 °C). The dielectric constant of the material was calculated using equation $\varepsilon' = Cd / (A\varepsilon_0)$. Where C is the capacitance of the sample, d is the thickness of the crystal, ε_0 is the permittivity of free space ($\varepsilon_0 \approx 8.854 \times 10^{-12}$ F / m) and A is the area of the sample. The variation of dielectric constant with frequency of CN crystal is shown in Fig. 7. From Fig. 7 it is observed that, the dielectric constant decreases with increasing frequency and reaches a constant value. The high value of dielectric constant at lower frequencies may be due to the contribution of all the four polarizations namely space charge, orientation, electronic and ionic polarizations and its low value at higher frequencies may be due to the loss of significance of these polarizations gradually [20]. The dielectric loss was calculated using the equation $\varepsilon'' = \varepsilon' \tan \delta$ and the variation of dielectric loss with varying frequency is depicted in Fig. 8. From the plot one can understand that the dielectric loss decreases with increase of frequency at different temperatures. The low dielectric loss value in high frequency for the sample suggests that the crystal has good optical quality and lesser defects.

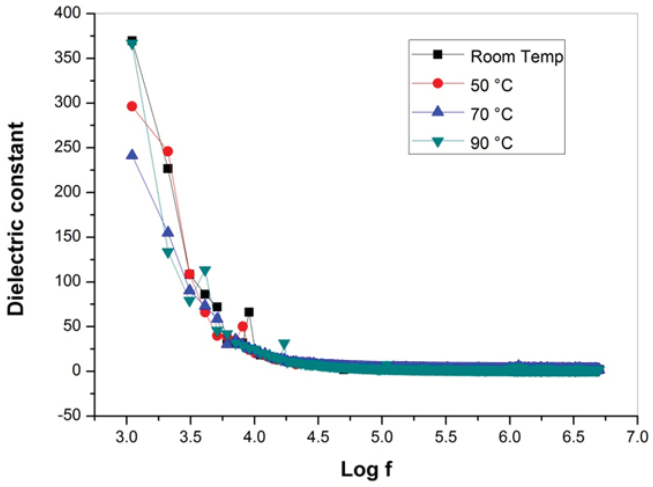

Figure 7: Frequency dependent dielectric constant of CN at various temperatures.

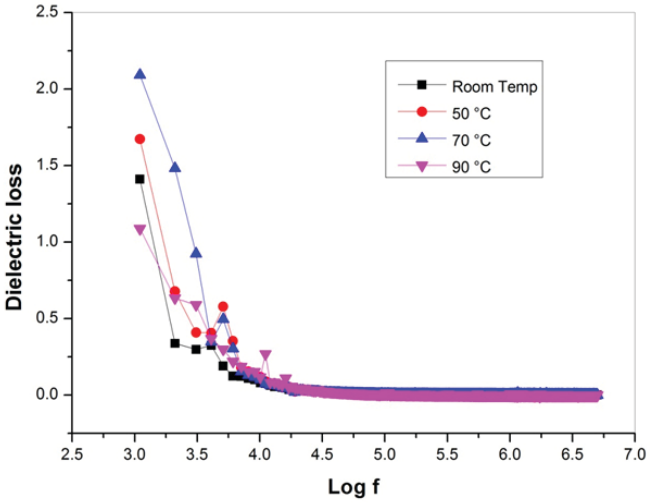

Figure 8: Frequency dependent dielectric loss of CN at various temperatures.

Photoluminescence study

Optical properties of the as grown CN single crystal were analyzed by photoluminescence spectroscopy. The near – band – edge photoluminescence of solids gives important information about the quality and composition of materials by probing the electron [21]. Photoluminescence is the ab-

sorption of photon energy promotes a valence electron from its ground state to an excited state. The excited energy is released as short wavelength light [22]. Photoluminescence of CN crystal is recorded with a Cary Eclipse fluorescence spectrometer (Type – Savitzky Golay) with auto excitation filter mode in the range 340 – 600 nm. The sample was excited at 320 nm. Photoluminescence spectrum of CN crystal is shown in Fig. 9. Spectrum shows a broad emission peaked at 378 nm which may be due to the vibrations in crystal lattice by changing incident power and sample temperature[23]. Intensity is slowly decreases in higher wavelength region. The result indicates that the emission of crystal is in violet region. The energy band gap of CN crystal has been calculated to be 3.2 eV using the formula Eg = 1240/ λ (eV)

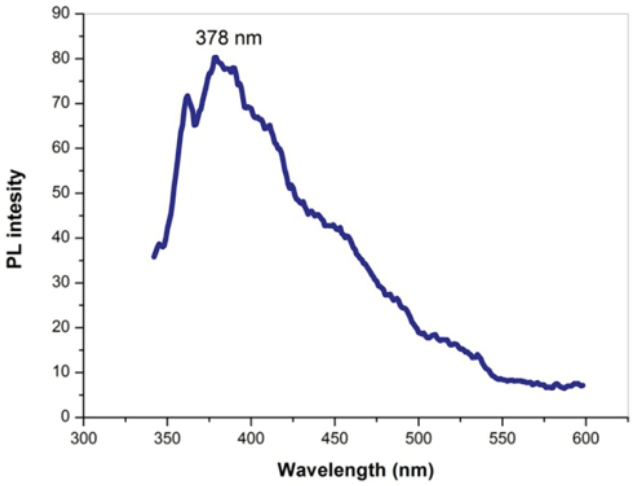

Figure 9: Photoluminescence spectrum of CN crystal.

Vickers microhardness analysis

For the commercial usage and device fabrication microhardness indentation analysis play a major role for conforming the mechanical stability. Microhardness studies were carried out on flat surface of the grown crystal of CN by using Shimadzu HMV-2000 hardness tester. Several trials of indentation were carried out for different loads (5g, 10g, 25g, 50g and 100g) at room temperature. Vickers hardness number (H_v) was calculated using the relation $H_v = 1.8544\ P/d^2$ (kg/mm^2), where P is the applied load in kg and d is the average diagonal length of indentation in mm. For loads above 100 g cracks started developing around the indentation impression. The variation of Vickers hardness values (H_v) with applied is shown in Fig. 10. Hardness (Hv) value increases with the increasing load. This type of variation of hardness is termed as reverse indentation size effect (RISE). In order to analyse the reverse indentation size effect (ISE), Meyers law was used by fitting the experimental data from the relation $P = Ad^n$, where P is the applied load, A is a constant, d is the average diagonal length of the indenter and n is the work hardening coefficient. By plotting log P versus log d (Fig.11), the value of work hardening coefficient (n) is calculated as 2.3. According to Onitsch [24], n lies between 1 and 1.6 for hard materials and for soft materials it is above 1.6. This implies that cytosinium nitrate belongs to soft material category.

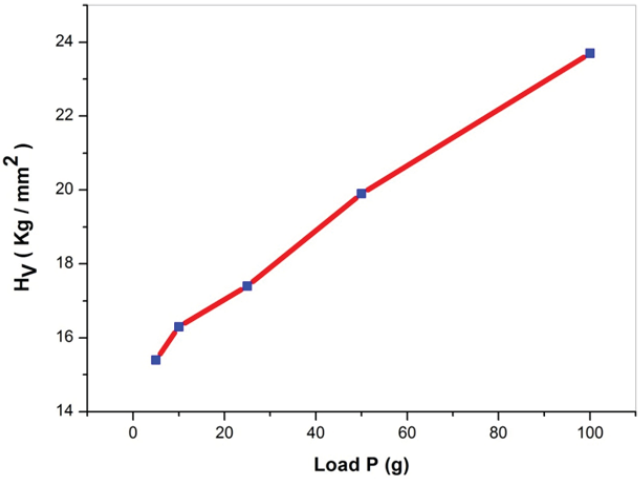

Figure 10: Variation of hardness number (H_v) Vs load (P) for CN crystal.

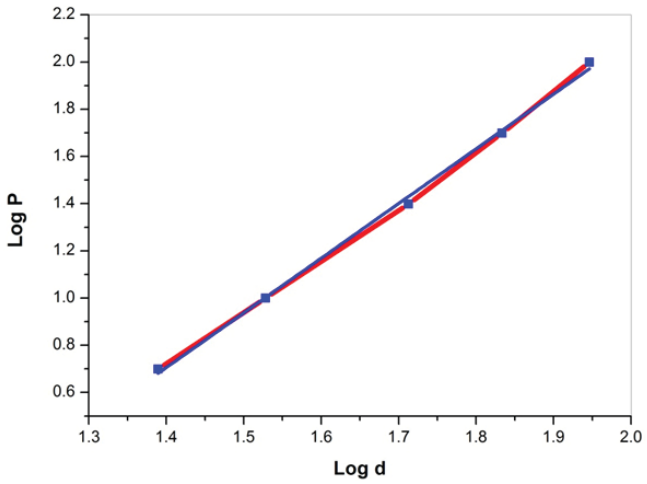

Figure 11: Variation of Log d Vs Log P for CN crystal.

Chemical etching analysis.

The microstructural analysis of the grown crystal by etching the surface gives more information about dislocations, imperfections and surface morphology. Optical behaviour of the NLO material in particular nonlinear efficiency mainly depends on the quality of the crystal. So it is very essential to study the surface morphology by etching of the as-grown crystal [25]. The etching of CN crystal was carried out by using double distilled water as an etchant. The cytosinium nitrate single crystal was immersed in water for few seconds and dried with tissue paper to remove the water molecules. The etch patterns in the crystal was examined using normal incident light type microscope. The photographs of etch

patterns were captured by Motic camera fitted with optical microscope. The microphotograph of CN crystal for etching time 5 s is shown in Fig. 12 (a). The figure shows predominant parallel ridges on crystal. Some of them extended over the surface while others are partly extended. Further the etching period was increased to 10 s and the etch pattern is shown in Fig. 12 (b). After etching for 10 s, the ridges were elongated in large number and forms different etch pattern. From the etching study there is such a periodicity seen in distribution of etch pattern.

Figure 12 (a): Etch pattern of CN single crystal (etching time 5 s).

Figure 12 (b): Etch pattern of CN single crystal (etching time 10 s).

Proliferation Assay

The synthesized cytosinium nitrate was evaluated for its anti-proliferative activity. For this, the cytosinium nitrate was tested for its anti-cancer properties on human lung cancer cell line A549. This assay was performed for determining the IC50. The cells were maintained in Dulbecco's modified Eagle's medium (DMEM) (Sigma-Aldrich Chemie Gmbh), supplemented with 10% fetal bovine serum (HyClone), 100IU/ml penicillin, 100mg/mL Streptomycin, and 2mmol/L L-glutamine (Sigma). Cells were seeded into 96-well plates at 5000 cells per well and incubated overnight. The medium was replaced with a fresh one containing the desired concentrations of CN dissolved in DMEM, ranging from 25µM, 50µM, 75µM, 100µM, 250µM and 500µM. Cells with cytosinium nitrate were incubated further for 24h and 48h. After treatment period, medium with cytosinium nitrate was removed and washed with 1XPBS (Phosphate buffered saline). Thereafter 100µl of MTT (3, 4, 5-dimethylthiazol-2yl)-2, 5-diphenyltetrazolium bromide)dye dissolved in serum free medium at the concentration of 5mg/mL, was added to the cells and incubated for 3h in CO_2 incubator. After 3h, the medium was removed and the formazan crystals were dissolved in 100µl of acidified isopropanol. The purple color of the formazan product was read in Robonik ELISA plate reader at 570nm. The percentage of cell viability was calculated with respect to control cells cultured at conditions similar to treated cells. Triplicate was maintained for all concentrations, including control cells.

Results indicate that cytosinium nitrate in the concentrations from 25µM to 250µM did not show any anti-cancer activity. Both control and treated cells have similar optical density upto 250µM. At 500µM concentration, a drastic decrease was observed in cell viability. At 24h, the viability was about 28%, which further decreased to 23% at 48h (Fig.13). This significant decrease may be due to the change in pH of the medium. At high concentrations such as above 250 µM, the nitric acid, component of cytosine nitric acid, induce change in pH towards acidicity. Change in color of the medium from pink to colorless even before the addition of MTT reagent for the MTT assay was probably the reason of cell death and cannot be considered due to toxicity of the compound *per se*. Study on the pharmacological effects of bioactive compounds on cancer treatments and prevention has increased dramatically over the past few decades. Many novel compounds, complexes of metals and heterocyclic combinations have been demonstrated to be cytotoxic and to possess anticancer activities in various cancer cells without exhibiting significant damage to normal cells [26 – 27]. In the present investigation, there was no significant toxicity demonstrated by the cytosine derivative at lower concentrations upto 250 µM, however, toxicity at 500 µM either did not seem to be evident due to its toxic nature, but due to high acidic nature of the compound itself. Cytosine being a significant bioactive molecule in its physiological perspective, it is believed by the authors that its modification further to make it toxic may provide a potential anti-cancer related bioactive molecule.

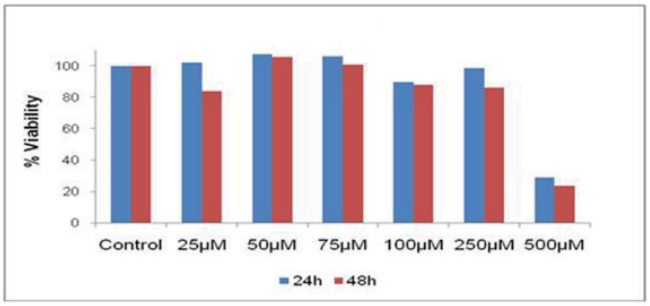

Figure 13: MTT assay for cytosinium nitrate against A549 cell line.

CONCLUSION

Cytosinium nitrate single crystals of size 7 mm × 2 mm × 1 mm were grown from aqueous solution by slow evaporation technique at room temperature. The grown crystal belongs to the triclinic system with centrosymmetric space group P_1. Various functional groups were present in the grown crystal was confirmed by FT IR analysis. It is evident from UV – Vis – NIR optical transmittance, the CN crystal has a wide transparency range in the entire UV visible and near infra red region. The low value of dielectric constant and dielectric loss of CN at higher frequencies revealed from dielectric measurements. The Vickers microhardness value increases with increase of load and shows reverse indentation size effect. The value of Meyer's index n turned out to be higher than 1.6 for CN and the material belongs to soft materials category. The variation of dielectric constant and dielectric loss were studied with varying frequency at different temperatures. Etching analysis shows the presence surface dislocations in the sample. The violet emission was identified by photoluminescence spectrum. Anticancer property was tested on human lung cancer cell line A549. No significant toxicity was demonstrated even by increasing concentrations.

ACKNOWLEDGEMENT

Authors acknowledge the immense help received from the scholars whose articles are cited and included in references of this manuscript. The authors are also grateful to authors / editors / publishers of all those articles, journals and books from where the literature for this article has been reviewed and discussed.

Financial support

The author Dr. T. Balakrishnan thanks the Council of Scientific and Industrial Research (CSIR), New Delhi, India for financial support [CSIR MRP.NO.3 (1314)/14/EMR-II, Dated 16.4.14].

Conflict of interest: Nil

Ethical approval: Not required

REFERENCES

1. J. Zyss, Molecular Nonlinear Optics: Materials, Physics and Devices, Academic Press, Boston, MA, 1994.
2. P.K. Hedge, A.V. Adhikari, M.C. Manjunath, C.S. Suchand Sandeep and R. Philip, Syn. Metals. 160 (2010) 1712–1717.
3. A. Philominal, S. Dhanuskodi and R. Philip, Curr. Appl. Phys. 12 (2012) 401–404.
4. S. Suresh, A. Ramanand, D. Jayaraman and P. Mani. Rev. Adv. Mater. Sci. 30 (2012) 175–183.
5. L. Liu, J. Ouyang and W.R.G. Baeyens, J. Chromotogr. A. 1193 (2008) 104-108.
6. D. L. Barker, and R. E.Marsh, Acta Cryst. 17 (1964) 1581-1587.
7. G. A. Jeffery, and Y. Kinoshita, Acta. Cryst. 16 (1963) 20-38.
8. B. Das, and J. B. Baruah, J. Mol. Struct. 1001 (2011) 134-138.
9. T. Lee, and P. Y. Wang, Cryst. Growth Des.10, (20 10) 1419–1434.
10. P.T. Muthiah, J.J. Robert, S.B. Raj, G. Bocelli and R. Olla, Acta. Crystallogr. Sect.E, 5 7 (2001) m558–m560.
11. D.T. Qui and M. Bagieu, Acta. Crystallogr., Sect.C, 46 (1990) 1645–1647.
12. B. Plitta, E. Adamska, M. Giel – Pietraszuk, A. Fedoruk – Wyszomirska, M. Naskret – Barciszewska, W. T. Markiewicz and J. Barciszewski. Eur. J. Med. Chem. 55 (2012) 243–254.
13. G. Portalone and M. Colapietro, J. Chem. Crystallogr. 39(2009) 193–200.
14. T.J. Kistenmacher, D.J. Szalda and L.G. Marzilli, Acta Cryst. B31 (1975) 2416–2422.
15. A.Cherouana, K.Bouchouit, L.Bendjeddou and N.Benali-Cherif, Acta. Crystallogr., Sect.E, 59 (2003) o983–o985.
16. B.K. Periyasamy, R.S.Jebas, N.Gopalakrishnan and T. Balasubramanian, Mater.Lett, 61 (2007) 4246–4249.
17. D. Kalaiselvi and R. Jayavel, Appl. Phys. A. 107 (2012) 93–100.
18. J. Tauc, Amorphous and liquid semiconductors, J. Tauc (Ed), Plenum, New York, 1974.
19. A.K.Chawla, D.Kaur and R.Chandra, Opt.Mater. 29 (2007) 995–998.
20. S. Suresh and D. Arivuoli, J. Miner. Mater. Char. Eng. 10 (2011) 517–526.
21. S.M. Dharmaprakash and P.Mohan Rao, J. Mater. Sci. Lett 8 (1989) 1167–1168.
22. A. Aravindan and P. Srinivasan, Cryst. Res. Technol. 11 (2007) 1097–1103.
23. G. Senthil Murugan and P. Ramasamy, Phys. B Condens. Matter, 406 (2011) 1169–1172.
24. E. M. Onitsch, Mikroskopie. 95,(1950) 12–14.
25. R. Ittyachan, P.C. Thomas, D.P. Anand, M.Palanichamy and P. Sagayaraj, Mater. Chem. Phys. 93 (2005) 272–276.
26. R.S. Katiyar, N.R. Kushwaha, R.V. Ramji Lal and N.Suryanarayana, Int. J. Agric. Cul. Sci. 4 (2009) 229–232.
27. S.K. Mantena, S.D.Sharma and S.K. Jatiyar. Mol. Canc. Therp. 5 (2006) 296–308.